

A Juxtamembrane Tyrosine in the Colony Stimulating Factor-1 Receptor Regulates Ligand-induced Src Association, Receptor Kinase Function, and Down-regulation*

Received for publication, December 24, 2003, and in revised form, August 2, 2004
Published, JBC Papers in Press, August 5, 2004, DOI 10.1074/jbc.M314170200

Cynthia M. Rohde, Jason Schrum, and Angel W.-M. Lee‡

From the Department of Pharmacology, University of Michigan Medical School, Ann Arbor, Michigan 48109

Recent literature implicates a regulatory function of the juxtamembrane domain (JMD) in receptor tyrosine kinases. Mutations in the JMD of c-Kit and Flt3 are associated with gastrointestinal stromal tumors and acute myeloid leukemias, respectively. Additionally, autophosphorylated Tyr⁵⁵⁹ in the JMD of the colony stimulating factor-1 (CSF-1) receptor (CSF-1R) binds to Src family kinases (SFKs). To investigate SFK function in CSF-1 signaling we established stable 32D myeloid cell lines expressing CSF-1Rs with mutated SFK binding sites (Tyr⁵⁵⁹-TFI). Whereas binding to I562S was not significantly perturbed, Y559F and Y559D exhibited markedly decreased CSF-1-dependent SFK association. All JMD mutants retained intrinsic kinase activity, but Y559F, and less so Y559D, showed dramatically reduced CSF-1-induced autophosphorylation. CSF-1-mediated wild-type (WT)-CSF-1R phosphorylation was not markedly affected by SFK inhibition, indicating that lack of SFK binding is not responsible for diminished Y559F phosphorylation. Unexpectedly, cells expressing Y559F were hyperproliferative in response to CSF-1. Hyperproliferation correlated with prolonged activation of Akt, ERK, and Stat5 in the Y559F mutant. Consistent with a defect in receptor negative regulation, c-Cbl tyrosine phosphorylation and CSF-1R/c-Cbl co-association were almost undetectable in the Y559F mutant. Furthermore, Y559F underwent reduced multiubiquitination and delayed receptor internalization and degradation. In conclusion, we propose that Tyr⁵⁵⁹ is a switch residue that functions in kinase regulation, signal transduction and, indirectly, receptor down-regulation. These findings may have implications for the oncogenic conversion of c-Kit and Flt3 with JMD mutations.

Colony stimulating factor-1 (CSF-1)¹ is an essential factor for monocyte/macrophage cell proliferation, differentiation, and

survival (1–3). Mice producing an inactive form of CSF-1 (Csf(*op*)/Csf(*op*)) exhibit osteopetrosis because of a decrease in osteoclasts as well as reduced numbers of monocytes and macrophages (4–6). They also have lower body weights, defects in reproduction, and a shorter lifespan. CSF-1 functions through a receptor tyrosine kinase (RTK), the CSF-1 receptor (CSF-1R), expressed on the surface of target cells. Recently, CSF-1R knockout mice were found to have a similar, but more severe phenotype, compared with the *op/op* mice, indicating that the CSF-1R is the main mediator of CSF-1 signaling (7).

CSF-1R is a member of the Class III RTK family, which also includes c-Kit, Flt3/Flk2, PDGFR α , and PDGFR β (8). These receptors are characterized by five immunoglobulin-like regions in the extracellular ligand-binding portion, a single spanning transmembrane region, a juxtamembrane domain (JMD), a kinase domain interrupted by a kinase insert (KI), and a carboxyl-terminal domain. Upon ligand binding, CSF-1R homodimerizes and autophosphorylates on six tyrosines in the cytoplasmic portion of the receptor. Tyr⁸⁰⁷ is located in the activation loop of the kinase domain (9) and its phosphorylation is important for kinase activity (10). The remaining tyrosines serve as binding sites for proteins containing Src homology 2 (SH2) binding domains. Three sites are found in the KI: Grb2/Mona (Tyr⁶⁹⁷) (11, 12), p85 subunit of phosphatidylinositol 3-kinase (Tyr⁷²¹) (13), and Stat1 (Tyr⁷⁰⁶) (14), the c-Cbl binding site is in the COOH terminus (Tyr⁹⁷⁴) (15, 16), and the Src family kinase (SFK) binding site is in the JMD (Y559) (17). These molecules further propagate the CSF-1 signal through activation of Ras/ERK, phosphatidylinositol 3-kinase/Akt, and STAT proteins. Two additional autophosphorylation sites have been described for *v-fms* (18, 19), the viral counterpart of the CSF-1R, but these have not been fully characterized for the CSF-1R. Precisely how the signal from the CSF-1R is transduced to these downstream targets and how they transmit the signal to the nucleus is not well understood.

Following ligand binding, the CSF-1R is rapidly internalized and degraded. This process begins with multiubiquitination of the CSF-1R mediated by c-Cbl (20), an E3-type ubiquitin ligase (21). CSF-1R presumably then migrates to clathrin-coated pits, is internalized through clathrin-mediated endocytosis, sorted into lysosomes, and degraded, as has been shown for other RTKs (22). c-Cbl appears to be important for both receptor internalization and degradation; c-Cbl overexpression leads to an increase in EGFR internalization (23, 24), whereas c-Cbl^{-/-} macrophages show a delay in CSF-1R internalization (20). c-Cbl may signal

* This work was supported by National Institutes of Health Grant RO1-CA85368 (to A. W.-M. L.). The costs of publication of this article were defrayed in part by the payment of page charges. This article must therefore be hereby marked "advertisement" in accordance with 18 U.S.C. Section 1734 solely to indicate this fact.

The atomic coordinates and structure factors (code 1RJB) have been deposited in the Protein Data Bank, Research Collaboratory for Structural Bioinformatics, Rutgers University, New Brunswick, NJ (<http://www.rcsb.org/>).

‡ To whom all correspondence should be addressed. Fax: 734-647-6202; E-mail: awmlee@umich.edu.

¹ The abbreviations used are: CSF-1, colony stimulating factor-1; CSF-1R, colony stimulating factor-1 receptor; EGFR, epidermal growth factor receptor; ERK, extracellular signal-regulated kinase; Flt3, Fms-like tyrosine kinase 3; GST, glutathione S-transferase; JMD, juxtamembrane domain; KI, kinase insert; PDGFR, platelet-derived growth factor receptor; RTK, receptor tyrosine kinase; SFK, Src family

kinase; SH2, Src homology 2; SHC, Src homology and collagen; SHIP, SH2-domain containing inositol 5'-phosphatase; TCL, total cell lysate; WT, wild-type; IL, interleukin; Stat, signal transducers and activators of transcription; ECD, extracellular domain; HRP, horseradish peroxidase; MTS, 3-(4,5-dimethylthiazol-2-yl)-5-(3-carboxymethoxyphenyl)-2-(4-sulfophenyl)-2H-tetrazolium, inner salt.

internalization through its interaction with CIN85, Cbl interacting protein of 85 kDa, an adapter molecule, and endophilin, a regulator of clathrin-mediated endocytosis (24, 25).

Recently, we showed that SFKs are activated by CSF-1 and serve as alternate activators of the Ras/ERK and phosphatidylinositol 3-kinase/Akt pathways in cells expressing a CSF-1R mutant lacking the KI (26). Several RTKs, including the CSF-1R (27), PDGFR β (28), c-Kit (29), and EGFR (30), activate SFKs, but it remains unclear what role these proteins play in RTK signaling. SFKs have been reported to activate the Ras/ERK, phosphatidylinositol 3-kinase/Akt, and STAT pathways (26, 31–33) as well as play a role in growth factor-induced cell cycle progression and *c-myc* transcription (34, 35). However, it has also been suggested that SFKs have a negative regulatory role in growth factor signaling, through reduction of Akt activity (36) or enhancement of c-Cbl activity (37). To investigate the role of SFKs in CSF-1 signaling, Tyr⁵⁵⁹ has been mutated in previous studies to Ala or Phe. The Y559A mutant showed normal *in vitro* kinase activity as well as normal ligand-induced receptor internalization (38). SFK binding was not investigated. The Y559F mutant exhibited decreased SFK binding, receptor phosphorylation and activity, and Stat3 phosphorylation (32). It is puzzling that mutation of the same residue to different amino acids should have such a different effect.

In addition to providing binding sites for interacting proteins, the JMD of RTKs may play a role in regulation of kinase function. Duplications, deletions, and point mutations in the JMD of Flt3 and c-Kit are commonly found in acute myeloid leukemias and gastrointestinal stromal tumors, respectively, causing constitutive receptor activation (39). Several lines of evidence support an autoinhibitory role of the JMD in RTKs. *In vitro* peptide binding studies demonstrate that unphosphorylated c-Kit JMD can inhibit its own kinase activity (40). X-ray crystal studies of the inactive, non-type III RTKs, Eph (41), and MuSK (42) as well as type III RTKs, Flt3 (43), and c-Kit (44) reveal that there is an intimate relationship between the JMD and the kinase domain. For example, in c-Kit, the closest relative to the CSF-1R, the JMD forms a hairpin that is partially buried in the interface between the NH₂- and COOH-terminal kinase lobes. This alters the position of a helix important for catalytic function (α C), prevents the activation loop from extending into an active conformation, blocks nucleotide binding, and allows Tyr⁸²³ to bind as a pseudosubstrate. It is easy to see how phosphorylation of the JMD tyrosines (Tyr⁵⁶⁸/Tyr⁵⁷⁰) can induce a conformational change that will disrupt some of the tight interactions between the JMD and kinase domain. In support of this possibility, the active c-Kit structure shows a vastly different conformation compared with the inactive structure (45).

To more fully elucidate the role of the JMD in CSF-1R signaling, we focused on the SFK binding motif. Stable IL-3-dependent 32Dcl23 cell lines expressing JMD CSF-1R mutants were established. In agreement with previous findings (17, 32), mutation of Tyr⁵⁵⁹ significantly reduced SFK binding. We also found that the Y559F mutant exhibited substantially decreased CSF-1-induced tyrosine phosphorylation, suggesting it may have a similar role as proposed for Tyr⁵⁶⁸/Tyr⁵⁷⁰ of c-Kit. Despite this decrease in receptor autophosphorylation, cells expressing Y559F displayed a CSF-1-dependent hyperproliferative phenotype. Y559F showed a marked reduction in c-Cbl binding, resulting in diminished CSF-1-induced c-Cbl tyrosine phosphorylation. Consistently, the Y559F mutant showed decreased CSF-1-induced multiubiquitination of Y559F and delayed receptor degradation. Consequently, Y559F and to a lesser extent Y559D, which exhibits an intermediate phenotype compared with the WT and Y559F receptors, transduced a low, but persistent activation of down-

stream signaling pathways, including Akt, ERK, and Stat5. Thus, hyperproliferation occurred as a result of the disruption of the balance between positive and negative signals. In summary, our studies support the model that the JMD of the CSF-1R has a dual role: autoinhibition in the unliganded state, and upon ligand binding and autophosphorylation, provision of docking sites for interacting proteins.

MATERIALS AND METHODS

Antibodies and Reagents—Cell culture reagents were from Invitrogen (Gaithersburg, MD) and Sigma. Recombinant human CSF-1 was a gift of the Genetics Institute (Cambridge, MA). Recombinant mouse IL-3 was purchased from Pepro Tech, Inc. (Rocky Hill, NJ). SU6656 and MG-132 were purchased from Calbiochem (La Jolla, CA). Chloroquine and methylamine were obtained from Sigma.

JMD peptides used in the competitive GST pull-down assay were synthesized by the University of Michigan Protein Structure Facility (Ann Arbor, MI). The JMD peptides, spanning residues 553–567 of the mouse CSF-1R, were synthesized with Tyr⁵⁵⁹ in the unphosphorylated or phosphorylated state. Peptides were dissolved in Me₂SO.

CSF-1R 422, 423, and 425 antibodies have been previously described (26) and the combination is referred to as anti-CSF-1R antibodies in the text. Anti-extracellular domain (ECD)-Fms (referred to as anti-ECD-Fms in the text) and anti-phosphotyrosine (Tyr(P)) (4G10) antibodies were purchased from Upstate (Lake Placid, NY); anti-Akt, Tyr(P) (PY99), ubiquitin, c-Cbl, Stat3, Stat5, GST, and Fyn antibodies were obtained from Santa Cruz Biotechnology, Inc. (Santa Cruz, CA); phospho-specific antibodies for CSF-1R, Akt, ERK, Stat3, and Stat5 were purchased from Cell Signaling Technology (Beverly, MA); anti-SHC antibodies were from Transduction Laboratories (San Diego, CA); anti-ERK and goat anti-mouse HRP antibodies were from Zymed Laboratories, Inc. (S. San Francisco, CA); donkey anti-rabbit HRP secondary antibody was from Amersham; and NeutrAvidin-HRP was from Pierce.

Cell Culture and Transfections—IL-3-dependent murine 32Dcl23 cells were cultured in RPMI 1640 medium supplemented with 10% fetal bovine serum and 5–10% WEHI-conditioned media as a source of IL-3. 32D cell lines expressing WT-CSF-1R have been previously described (46). The JMD CSF-1R mutants were constructed by replacing the internal StuI fragment of the murine CSF-1R cDNA with the corresponding fragment containing point mutations, produced using a two-step PCR method (47). All PCR-amplified segments were sequenced in their entirety and on both strands. The CSF-1R mutant cDNAs were inserted into pMSCV-IRES-puro and transiently transfected into BOSC23 cells. Viral supernatants obtained after 48 h were used to transduce 32Dcl23 cells. Clones were selected using 1 μ g/ml puromycin and screened by ¹²⁵I-CSF-1 binding as described (26). JMD clones designated as (lo) expressed similar receptor levels as the WT (hi) clone, which was used as a control in all experiments except where indicated. JMD clones described as (hi) expressed higher levels (~1.5–2-fold) of receptors compared with the WT (hi) clone. Unless otherwise indicated, JMD (lo) clones were used in all experiments. For clones of interest, RNA was extracted, reverse transcribed, and the sequence of the JMD verified.

Protein Analysis—Except where noted, immunoprecipitation and immunoblotting were performed as described (26). Equal amounts of protein as determined by the Bio-Rad protein assay were loaded for each immunoblot of total cell lysate (TCL) as shown. In all cases, quantitation of receptor levels in receptor immunoprecipitations was carried out on duplicate samples subjected to the same processing. For most experiments, the anti-ECD-Fms antibody was used to immunoprecipitate the CSF-1R. Western blots of the receptor were probed sequentially with anti-ECD-Fms and then anti-CSF-1R (422/423/425) antibodies to eliminate possible differences in antibody recognition. For downstream substrate activation experiments, cells (2 \times 10⁶/ml) were starved for 3 h in a 24-well plate. Cells were left unstimulated or stimulated with 10 nM CSF-1 for the times indicated in the figures and then transferred to ice-cold Hanks' balanced salt solution containing 0.2 mM Na₃VO₄. After two washes, cells were lysed as described (26). For CSF-1R kinase assays, lysates from starved cells were first pre-cleared by incubation with rabbit serum-bound protein A-Sepharose for 45 min. Then, lysates were incubated with anti-ECD-Fms pre-bound to protein A-Sepharose for 6 h at 4 °C with rocking, followed by extensive washing of the immune complexes. The complexes were incubated for 20 min at 30 °C in kinase buffer (20 mM Hepes, 10 mM MnCl₂, 1 mM dithiothreitol, 1 mM Na₃VO₄) containing 200 μ M ATP. The kinase assay buffer was removed and the beads were washed once with HBS (25 mM Hepes, 150 mM NaCl, 1 mM dithiothreitol) supplemented with protease and phosphatase inhibitors. The reaction was stopped by addition of 2 \times Laemmli

buffer and boiled. Proteins were separated using SDS-PAGE, transferred to polyvinylidene difluoride (Millipore) and immunoblotted as described in the figure legends. For CSF-1R/c-Cbl co-immunoprecipitation experiments, cells were either treated with methylamine or chloroquine, in combination with MG-132, for 1 h prior to CSF-1 stimulation at 37 °C, or cells were stimulated at 4 °C for 20 min. Lysis was with an equal volume of 2× TNE lysis buffer (20 mM Tris, pH 7.8, 300 mM NaCl, 2 mM EDTA, 0.2% Nonidet P-40) as previously described (48) and supplemented with protease and phosphatase inhibitors. 750 µg of cell lysate was incubated with anti-ECD-Fms or anti-c-Cbl antibodies followed by capture with protein A-Sepharose beads. After extensive washing, 2× Laemmli was added; the samples were boiled and analyzed by SDS-PAGE and immunoblotting. Quantitation of immunoblot results was carried out as described previously (26) by scanning multiple exposures with Adobe Photoshop 7.0 and quantitating band intensities with NIH Image 1.62 software.

GST Pull-down Assay—GST pull-down assays were performed essentially as previously described (26). Pre-cleared 32D cell lysates were incubated with 5 µg of GST or GST-Fyn-SH2 bound to GSH-Sepharose (Amersham Biosciences) for 3 h at 4 °C with rocking followed by extensive washing of complexes. Bound proteins were eluted by boiling in 2× Laemmli. CSF-1R proteins were separated by SDS-PAGE and detected by immunoblotting with anti-ECD-Fms antibodies. Peptide competition assays were performed as described above except that, after pre-clearing, the lysates were incubated with Me₂SO or the indicated amount of unphosphorylated or phosphorylated JMD peptide at 4 °C for 1 h before incubation with GST-Fyn-SH2.

Biotinylation and Internalization Assay—After stimulation, cells were immediately placed on ice and washed multiple times with ice-cold phosphate-buffered saline, pH 7.8. Cells were incubated with 0.5 mg/ml NHS-PEO₄-Biotin (Pierce) for 1 h at 4 °C to label the remaining cell surface proteins. The biotinylation reaction was stopped by incubating cells with stop buffer (phosphate-buffered saline, pH 7.8, containing 10 mM glycine) for 10 min at 4 °C. Cells were washed again with stop buffer and then lysed with 1× lysis buffer supplemented with protease and phosphatase inhibitors. CSF-1Rs were immunoprecipitated from cell lysates. Immune complexes were sequentially blotted with anti-CSF-1R antibodies, to determine receptor degradation, and with NeutrAvidin-HRP, to detect CSF-1Rs remaining on the cell surface after stimulation.

Cell Proliferation Studies—Cells were washed multiple times (1× with RPMI, 2% fetal bovine serum, and 2 times with Hanks' balanced salt solution) before seeding at 7.5 × 10⁴ cells/ml in 96-well plates in RPMI, 10% fetal bovine serum. Unless otherwise indicated, 10 nM CSF-1 or 5 ng/ml recombinant murine IL-3 were added to each well. Cells were split 1:10 every 2 days into fresh media supplemented with the appropriate growth factor and studies were carried out for 6 days. Living cells were counted every 24 h using trypan blue exclusion and a hemocytometer. Additionally, an MTS assay (Cell Titer 96 AQueous Cell Proliferation Assay; Promega, Madison, WI) was performed every day according to the manufacturer's instructions, to test for metabolically active cells. For SU6656 growth studies, cells were pretreated with SU6656 for 1 h before addition of CSF-1. MTS activity was analyzed after 48 h.

CSF-1R Modeling—The JMD and kinase domain of the mouse CSF-1R were modeled on the autoinhibited FLT3 structure (Protein Data Bank code 1RJB) using SWISS-MODEL (version 36.0003) (49–51).

Statistical Analysis—*p* values were calculated using the Student's *t* test (2-sided).

RESULTS

Mutation of Tyr⁵⁵⁹ Significantly Reduces SFK Association with CSF-1R—To investigate the role of SFK in CSF-1 signaling, we performed a mutagenesis study of the SFK binding site in the JMD of the CSF-1R (Fig. 1A). Investigations of the PDGF, Eph, and MuSK receptors point to an additional, auto-inhibitory role for the JMD (41, 42, 52–54). Taking into account this possibility, we made three point mutants. A Tyr to Phe substitution at residue 559 is predicted to eliminate binding by the SH2 domain of SFKs but at the same time may lock the receptor in an inactive conformation, a possibility proposed for analogous mutations in the Eph receptor (55). A Tyr to Asp mutation at residue 559 is also predicted to eliminate SFK binding, as high affinity binding requires an amino-aromatic interaction between the phosphate group and a buried arginine at the bottom of the binding pocket. The side chain of the

aspartic acid is too short to allow the carboxyl group to reach the terminal nitrogen on arginine (56). However, the negative charges on the aspartic acid may induce a phosphomimetic state and avoid an inhibitory effect of the JMD on kinase function. Lastly, an Ile to Ser mutation was introduced at the Tyr(P) +3 position. Structural studies (56) and peptide library screening (57) indicate that the SH2 domain of SFKs prefers a residue with a large hydrophobic side chain in the Tyr(P) +3 position. Hence the I562S substitution is predicted to decrease SFK binding but to allow Tyr⁵⁵⁹ to undergo autophosphorylation. All clones were stably expressed in IL-3-dependent murine 32Dc123 cells and shown to bind ¹²⁵I-CSF-1 under saturation binding conditions (data not shown).

To investigate the ability of WT-CSF-1R and the JMD mutant receptors to bind SFKs in response to CSF-1, a GST pull-down assay was performed using the SH2 domain of Fyn (Fig. 1B). We examined the association of total CSF-1R protein with SFKs, unlike a previous investigation that only determined association of tyrosine-phosphorylated CSF-1R (32). The results confirmed that WT-CSF-1R associated with GST-Fyn-SH2 only after CSF-1 stimulation and did not bind to GST alone. Similar results were obtained with GST-Src-SH2 and GST-Yes-SH2 (data not shown). The association between CSF-1R and Fyn could be competed away by a phosphorylated, but not an unphosphorylated, peptide corresponding to the SFK binding site (Fig. 1C), establishing that Tyr⁵⁵⁹ can function as an SFK binding site *in vitro*. Although the GST-Fyn-SH2 interaction with Y559D and Y559F was significantly reduced, it was not abolished suggesting the possibility of a minor SFK binding site that was revealed by the mutation. Surprisingly, I562S showed only a slight decrease in Fyn binding, compared with the WT receptor, indicating that I562S in the Tyr(P) +3 position may not be as important for SFK binding as previously thought (56, 57).

Y559F Displays Decreased Tyrosine Phosphorylation Independent of Src Kinase Activity—In addition to serving as a binding site for interacting proteins, the JMD of RTKs may also function in kinase regulation (41–44, 52). To investigate this hypothesis, we examined several indicators of receptor kinase activity. Ligand-induced RTK autophosphorylation is generally accepted as a reflection of kinase activity. The WT (Fig. 2A) and I562S (data not shown) receptors exhibited a transient increase in autophosphorylation after CSF-1 stimulation. After correcting for receptor levels, Y559D autophosphorylation was modestly decreased (by 23–30% at 1 min and by 53–60% at 5 min (*n* = 3)), compared with WT (Fig. 2A), implying that the Tyr to Asp substitution may partially mimic phosphorylated Tyr and permit kinase activation. Y559D was basally phosphorylated in the experiment shown; however, this finding was variable, indicating that the Tyr to Asp substitution in itself was insufficient to constitutively activate the receptor. In contrast, Y559F autophosphorylation was significantly reduced (by 70–80% at 1 min and ≥90% at 5 min (*n* = 3)) indicating that Y559F has reduced CSF-1-induced kinase activity. This reduction in Y559F autophosphorylation was not because of low cell surface expression as ¹²⁵I-CSF-1 binding studies in living cells confirmed cell surface expression of all of the mutant receptors (data not shown), and Western blotting showed an appropriate ratio of the mature receptor to its precursor (Figs. 1B, 2, 6, and 7).

Phosphorylation at the activation loop tyrosine(s) is a prerequisite for enhancement of kinase activity in many RTKs, including the CSF-1R (10, 58). To examine *in vivo* kinase function, we used an antibody that specifically recognizes phosphorylated Tyr⁸⁰⁷ in the activation loop. When normalized to total receptor levels, Tyr⁸⁰⁷ phosphorylation in the Y559F mutant was reduced by ~90% (*n* = 2) of that observed

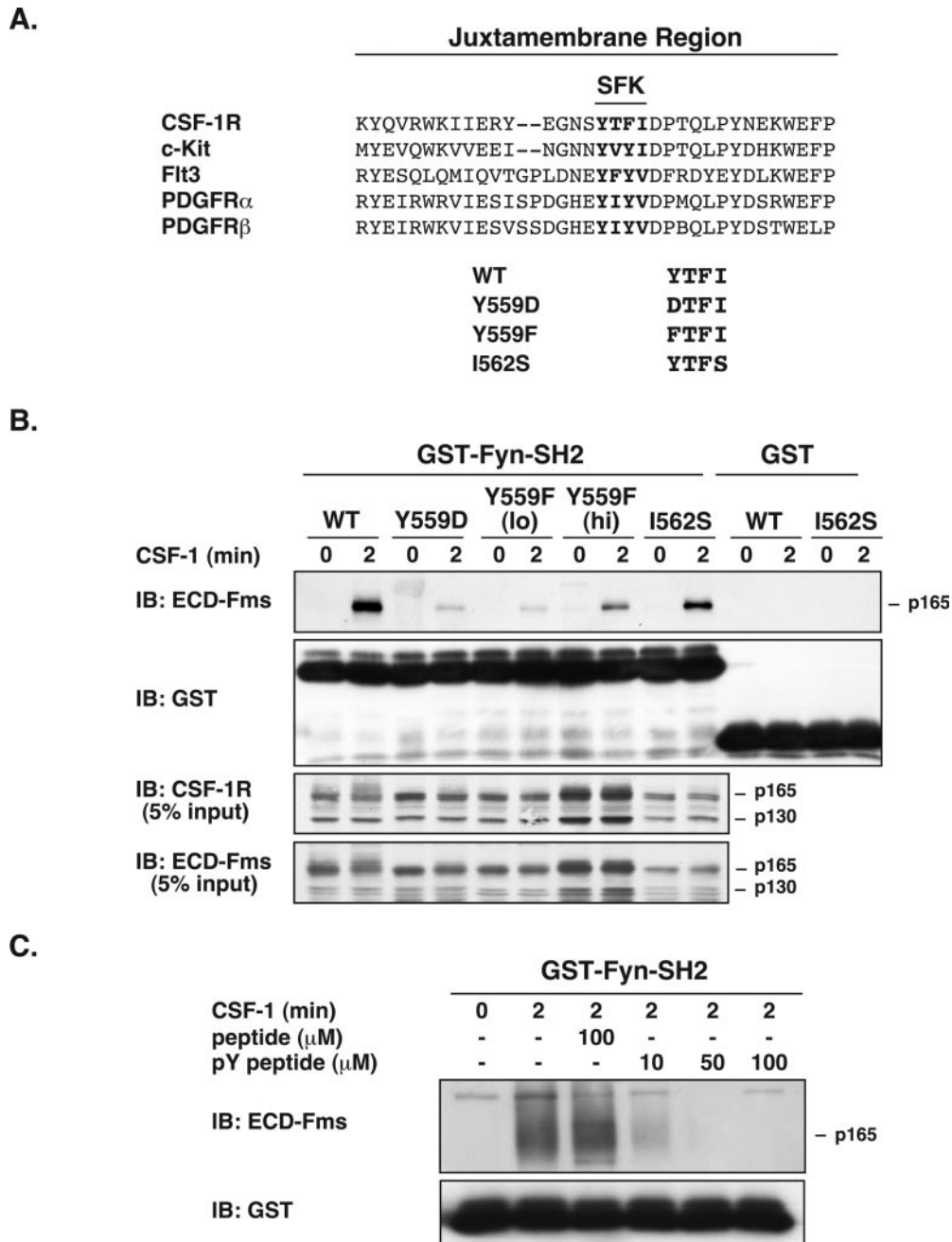


FIG. 1. Mutation of the SFK binding site in the JMD reduces association of CSF-1R with Fyn. *A*, SFK binding site mutants. Shown is an alignment of the JMD from type III RTKs. The SFK binding site is in **boldface**. The mutants used in this study are indicated. *B*, CSF-1R association with Fyn. Lysates from unstimulated cells or cells stimulated with CSF-1 for 2 min were incubated with either GST or GST-Fyn-SH2 in a GST pull-down assay. CSF-1R:GST-Fyn-SH2 complexes were analyzed by immunoblotting with anti-ECD-Fms (*top panel*). The blot was stripped and reprobed with anti-GST to verify equal amounts of fusion protein in the assay (*second panel*). Equal amounts of TCLs are shown as a control for receptor levels. Parallel blots of TCLs were probed with either anti-CSF-1R (*third panel*) or anti-ECD-Fms (*fourth panel*) antibodies to demonstrate reproducibility between the different antibodies. Shown is a representative experiment out of three. *C*, peptide competition. Cells were left unstimulated or stimulated for 2 min with CSF-1. Lysates were incubated with the indicated amount of unphosphorylated or phosphorylated JMD peptide and then used in a GST pull-down assay with GST-Fyn-SH2. Complexes were analyzed by immunoblotting with anti-ECD-Fms (*top panel*). The blot was stripped and reprobed with anti-GST to verify equal amounts of fusion protein in the assay (*bottom panel*). Shown is a representative experiment out of two.

for the WT-CSF-1R (Fig. 2*B*). Tyr⁸⁰⁷ phosphorylation was more modestly reduced in the Y559D mutant, by 50–60% ($n = 2$) (Fig. 2*B*). To determine whether the JMD mutants have an intrinsic kinase defect, an *in vitro* kinase assay was performed on CSF-1R immunoprecipitates isolated from unstimulated cells. When activated with 200 μ M ATP and 10 mM MnCl₂, there was little difference in the ATP-inducible kinase activity of the different CSF-1Rs, as measured by the pY807-CSF-1R antibody (Fig. 2, *C* and *D*). Thus, the WT

receptor and JMD mutants have similar intrinsic kinase activities; hence, the inability of Y559F to autophosphorylate is ligand-dependent, consistent with the possibility that the JMD in the CSF-1R has an autoinhibitory role.

It remains a possibility that SFKs could phosphorylate the CSF-1R and the reduction in Y559F phosphorylation is because of ablated SFK recruitment by Y559F. To test this possibility, we examined CSF-1-induced receptor phosphorylation after pretreatment of cells with the specific SFK inhibitor SU6656

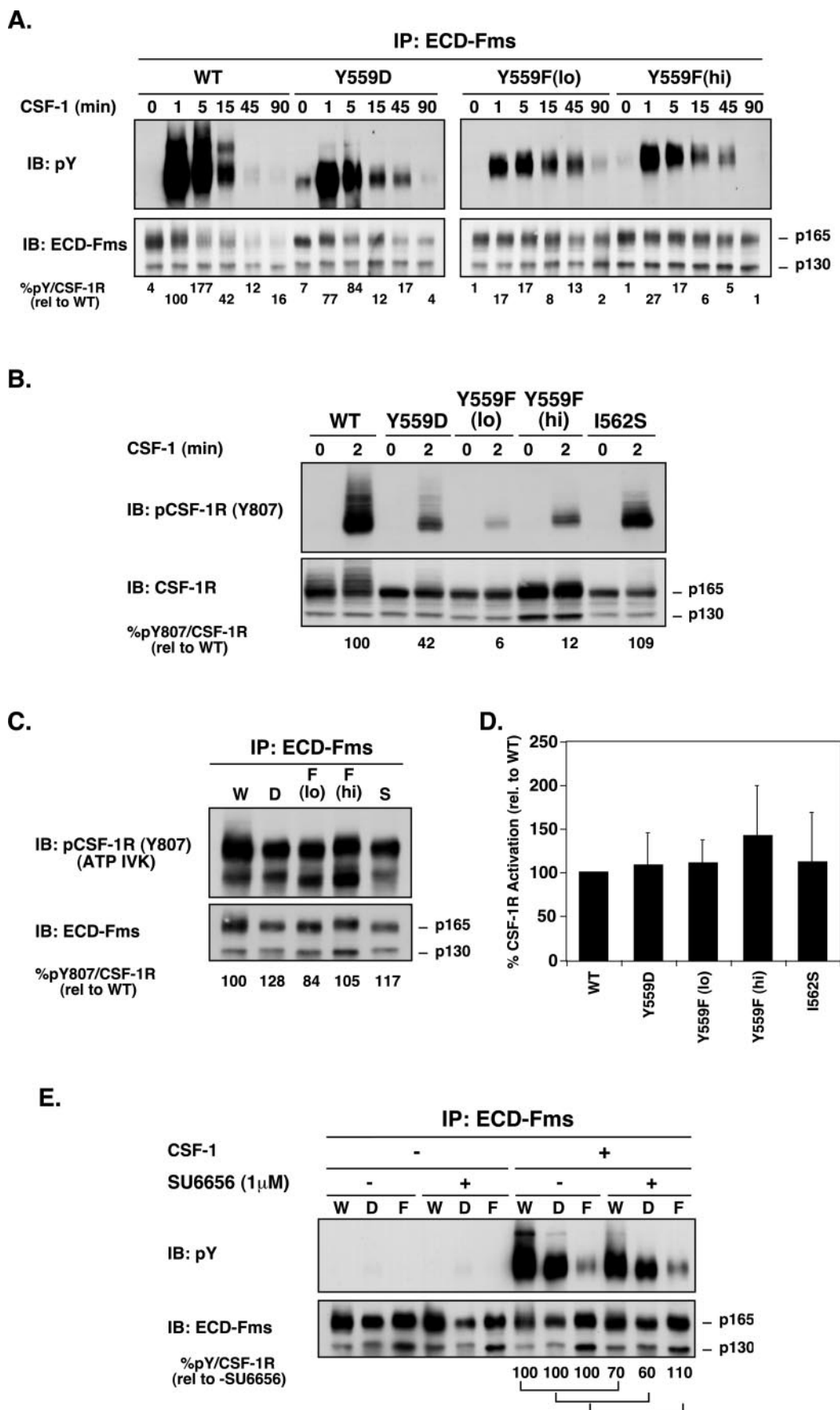


FIG. 2. Y559F displays decreased tyrosine phosphorylation independent of loss of SFK binding. A, CSF-1R tyrosine phosphorylation in response to CSF-1. Cells were stimulated for the indicated times. Lysates were immunoprecipitated with anti-ECD-Fms antibodies. Immunoprecipitations were performed in duplicate, one set blotted with anti-Tyr(P) and the second set with anti-ECD-Fms antibodies. Shown is a representative experiment out of four. Levels of tyrosine phosphorylation were quantitated (see "Materials and Methods") and normalized to total

(59). SU6656 treatment did not have a dramatic effect on the autophosphorylation of WT, Y559D, or Y559F receptors (Fig. 2E), indicating that SFKs are unlikely to significantly phosphorylate the CSF-1R. Instead these results imply that Tyr⁵⁵⁹ functions as a switch residue to regulate receptor kinase activity in response to ligand.

Cells Expressing Y559F Exhibit a Hyperproliferative Phenotype—As CSF-1 is a potent growth factor for cells of the monocyte/macrophage lineage, we evaluated the ability of the CSF-1R mutants to mediate 32D cell proliferation in response to CSF-1. 32D cells depend on IL-3 for growth and survival. They do not express the CSF-1R endogenously, but can switch to CSF-1-dependent proliferation in the absence of IL-3 if the CSF-1R is expressed exogenously. Proliferation was measured by two assays: doubling time, calculated from viable cell counts over 6 days of growth in CSF-1, and MTS activity, determined after 3 days of growth in CSF-1. Parallel experiments were carried out in IL-3. Two clones per construct were analyzed. To eliminate clonal variations, results for proliferation in CSF-1 were calculated as a percent of growth measured in parallel samples cultured in IL-3. Compared with cells expressing the WT receptor, cells expressing the Y559F receptor exhibited a significant decrease in doubling time (Fig. 3A) and a concurrent increase in MTS activity (Fig. 3B). This hyperproliferation was observed over a range of CSF-1 concentrations (Fig. 3C). Although cells expressing Y559D displayed a trend toward decreased doubling times and increased MTS activity, this increase in cell proliferation was statistically significant only for the Y559D (hi) cells, consistent with the Y559D mutant having an intermediate phenotype. Cell lines expressing I562S displayed growth profiles similar to cells expressing the WT-CSF-1R in response to CSF-1 (Fig. 3, A and B). A previous study in M1 myeloid cells attributed the hyperproliferation of cells expressing the Y559F receptor to a decreased ability to differentiate in the presence of CSF-1 (32). However, as 32D cells expressing WT-CSF-1R do not exhibit signs of differentiation (as assessed by morphological changes, cell attachment, or cell surface markers such as Mac1), we conclude that reduced differentiation is not the cause of the Y559F hyperproliferative phenotype.

Loss of SFK binding predicts that CSF-1-dependent proliferation of cells expressing Y559D or Y559F would be insensitive to SFK inhibition. Cells expressing the WT-CSF-1R, Y559D, or Y559F were pretreated with increasing concentrations of SU6656 for 1 h before CSF-1 stimulation and MTS activity was examined after 48 h. Cells expressing the WT-CSF-1R showed a dramatic decrease in proliferation after SU6656 treatment (Fig. 3D) with an IC₅₀ value of 0.4 μM, very similar to the reported IC₅₀ values for Src, Fyn, Lyn, and Yes (59). These results indicate that SFK activity is required for CSF-1-mediated proliferation in myeloid cells. In agreement with our prediction, the Tyr⁵⁵⁹ mutants were not affected by SU6656 treatment except at significantly higher doses where SU6656 could be affecting other kinases (Fig. 3D), thus confirming that the Y559F hyperproliferative phenotype is SFK-independent.

Positive Regulators of Cell Proliferation and Survival Downstream of Tyr⁵⁵⁹ Mutants—Cell proliferation in response to growth factors and cytokines is determined by a balance between the activities of positive and negative regulators (8). To identify the mechanism underlying the increase in Y559F proliferation, we investigated the activation of a number of pro-mitogenic regulators. Previously, we had demonstrated a good correlation between Akt and ERK kinase activity and their phosphorylation status (26). Furthermore, tyrosine phosphorylation of STAT proteins is important for their dimerization and nuclear translocation (60). Therefore, we used phospho-specific Akt, ERK, and Stat3/5 antibodies to determine the activity of each protein. A trend toward increased CSF-1-induced ERK phosphorylation, and to a lesser extent Akt phosphorylation, was observed in cells expressing the Y559F mutant compared with the WT clone during the initial stages of activation (Fig. 4, A and B). Stat5 tyrosine phosphorylation also evidenced a trend of increased activation mainly in cells expressing Y559F (hi) (Fig. 4, A and B). The mobility shift observed for Stat5, which is not represented in the quantitation, was most likely due to both tyrosine and serine phosphorylation because at later time points a mobility shift was still observed, although tyrosine phosphorylation had abated. Serine phosphorylation of Stat5 is known to occur in response to various cytokines and appears to be necessary for optimal transactivation of target gene expression (61). CSF-1-stimulated phosphorylation of Stat3 was markedly reduced in the Y559F (lo), but not Y559F (hi), clone (Fig. 4, A and B), presumably because of the significant difference in receptor numbers (Figs. 1B and 2B). Notably, Stat3 tyrosine phosphorylation was preserved in the Y559D mutant. In separate experiments, we found that CSF-1-induced Stat3 phosphorylation was significantly diminished by treatment of 32D cells expressing WT-CSF-1R with SU6656 or another SFK inhibitor, PP2.² This is supported by previous reports that Stat3 may be a direct Src substrate (62). To reconcile our observations, we propose that there are multiple pathways utilized by the CSF-1R to mediate Stat3 activation: pathways that depend on recruitment of SFKs to Tyr⁵⁵⁹ and those that do not, but require CSF-1R autophosphorylation. Presumably, the elimination of SFK binding, coupled with significantly reduced receptor autophosphorylation, as well as the relatively lower number of Y559F receptors in Y559F (lo) cells, account for the almost complete absence of Stat3 phosphorylation in Y559F (lo) cells.

The adapter SHC undergoes tyrosine phosphorylation in response to a variety of stimuli, including CSF-1. Additionally, SHC is a substrate of SFKs (59) and appears to play an important role in the proliferation of an EGFR mutant lacking several autophosphorylation sites in the carboxyl terminus (63). We observed a marked decrease in CSF-1-dependent SHC phosphorylation in cells expressing the Y559F mutant (Fig. 4C). In WT cells, SHC associated inducibly with SH2-domain

² C. M. Rohde and A. W. Lee, unpublished observations.

receptor levels. Results are presented as relative to WT tyrosine phosphorylation. B, phosphorylation of the Tyr⁸⁰⁷ residue of CSF-1R in response to CSF-1. Cells were left unstimulated or stimulated for 2 min. Lysates were analyzed by blotting with anti-phospho-CSF-1R (Tyr⁸⁰⁷) or anti-CSF-1R. Results were quantitated as described in A. Shown is one out of two experiments. C, CSF-1R *in vitro* kinase assay. Unstimulated cell lysates were immunoprecipitated with anti-ECD-Fms antibodies and used in an *in vitro* kinase assay in the presence of 200 μM ATP and 10 mM MnCl₂. Shown is a representative experiment out of four. Results were quantitated as described in A. D, quantitation of ATP-induced *in vitro* CSF-1R activation. *In vitro* kinase data as described in C was quantitated. Results from Tyr⁸⁰⁷ blots were normalized to total receptor levels and then expressed as a percentage of WT-CSF-1R activation. Shown is the average ± S.D. (n = 4). E, SU6656, an SFK-specific inhibitor, does not dramatically affect CSF-1R tyrosine phosphorylation. Cells were pretreated for 1 h with SU6656 and then left unstimulated, or stimulated with CSF-1 for 1 min. Lysates were immunoprecipitated with anti-ECD-Fms antibodies and parallel immunoprecipitates were analyzed by probing with anti-Tyr(P) or anti-ECD-Fms antibodies. Shown is a representative experiment out of two. Levels of tyrosine phosphorylation were quantitated and normalized to total receptor levels. Results are presented relative to CSF-1-induced receptor tyrosine phosphorylation in the absence of SU6656. Abbreviations in the figure are: W, WT-CSF-1R; D, Y559D; and F, Y559F (hi).

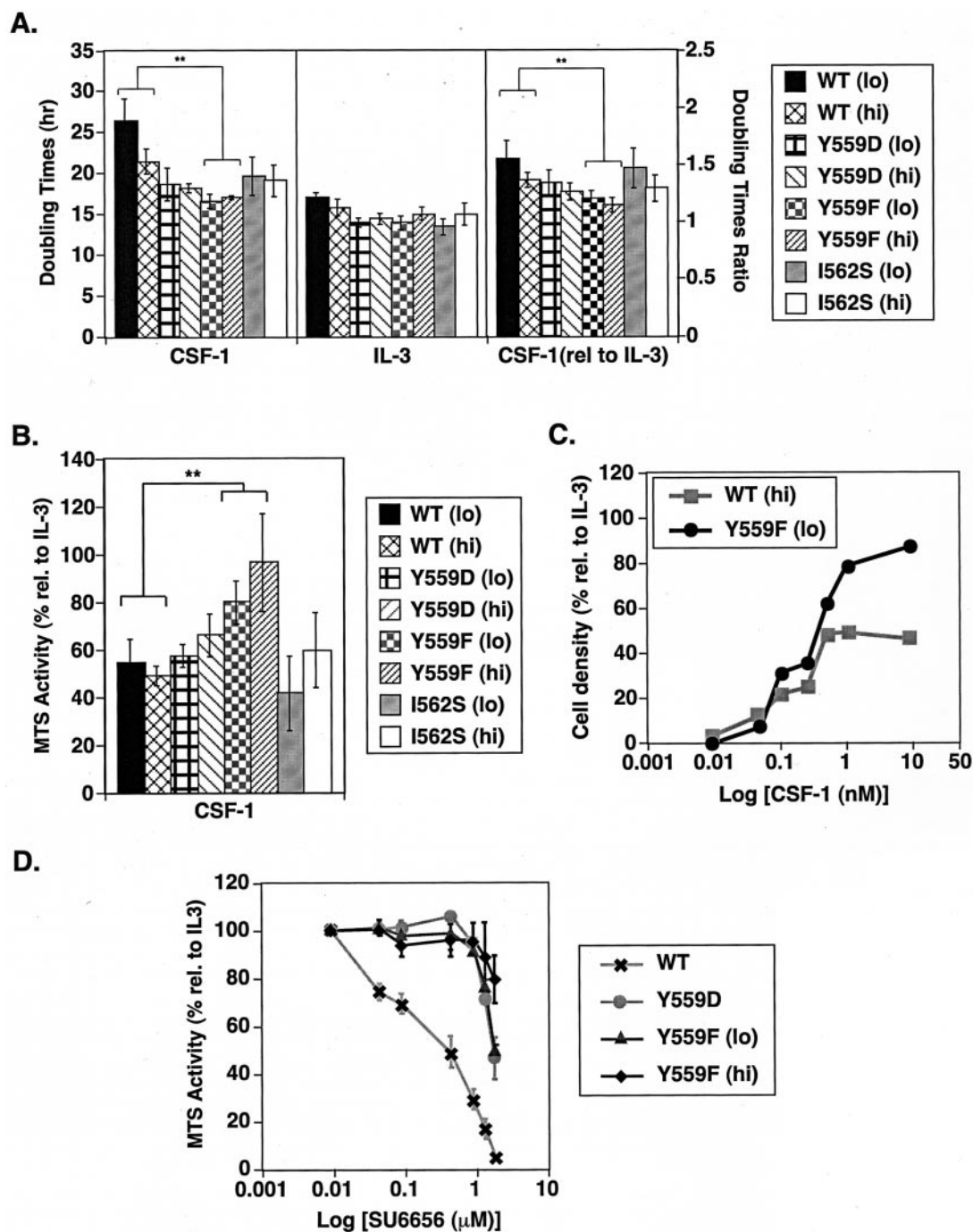


FIG. 3. Cells expressing Y559F exhibit a hyperproliferative phenotype. Cells expressing WT or JMD mutant CSF-1Rs were seeded in RPMI, 10% fetal bovine serum with either CSF-1 or IL-3. *A*, doubling times. *Left, middle panels*, doubling times of cells grown in either CSF-1 or IL-3 were calculated based on a 6-day growth curve. *Right panel*, doubling times for CSF-1 were normalized to doubling times of IL-3. Only Y559F doubling times were statistically different (**, $p < 0.005$) compared with WT. *B*, MTS activity. MTS activity was measured 3 days after growth factor stimulation. *Graph* indicates the average \pm S.D. ($n = 6$). Y559F exhibited a statistically significant (**, $p < 0.005$) increase in MTS activity over WT. *C*, CSF-1 dose dependence of cell proliferation. Cells expressing WT and Y559F receptors were grown in the presence of increasing amounts of CSF-1. Results show cell densities after 3 days when normalized to cell densities achieved in IL-3. Shown is a representative of two independent experiments. *D*, dose-dependent effect of SU6656 on cell proliferation. Cells expressing the WT or JMD mutant CSF-1Rs were pretreated with the indicated SU6656 concentrations for 1 h before growth factor stimulation. MTS activity was monitored after 48 h. The *graph* indicates average \pm S.D. ($n = 2$).

containing inositol 5'-phosphatase (SHIP) as shown previously (64). In Y559F cells, the decrease in SHC tyrosine phosphorylation was accompanied by a decrease in associated tyrosine-phosphorylated SHIP (Fig. 4C). Compared with Y559F (lo), the Y559D clone exhibited a less severe reduction of SHC tyrosine phosphorylation and associated tyrosine-phosphorylated SHIP. For reasons that are not entirely clear, the amount of tyrosine-

phosphorylated SHIP associated with SHC in Y559D-expressing cells was variable, but always less than WT. Because SHIP hydrolyzes phosphatidylinositol-(3,4,5)-trisphosphate to phosphatidylinositol-(3,4)-bisphosphate, the possibility exists that diminished SHIP recruitment to Y559F could contribute to the hyperproliferative phenotype, although this marked decrease is not reflected in dramatically enhanced Akt activation during

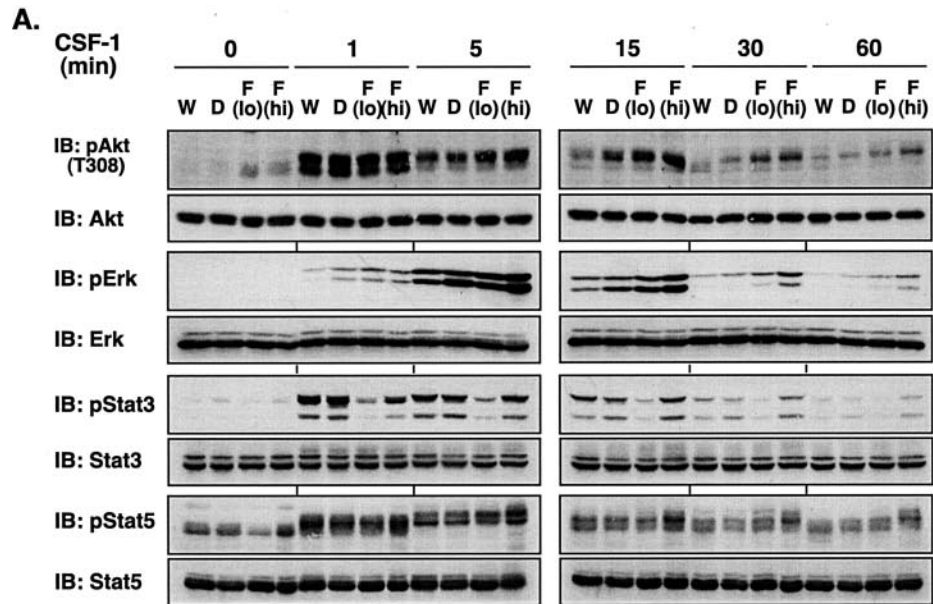
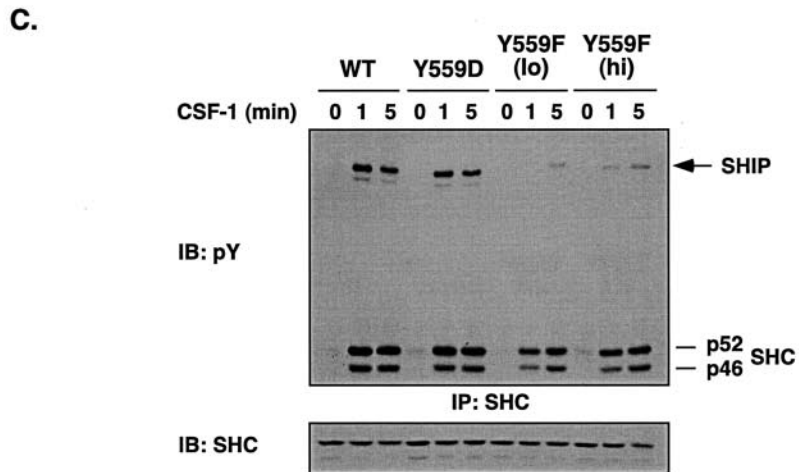
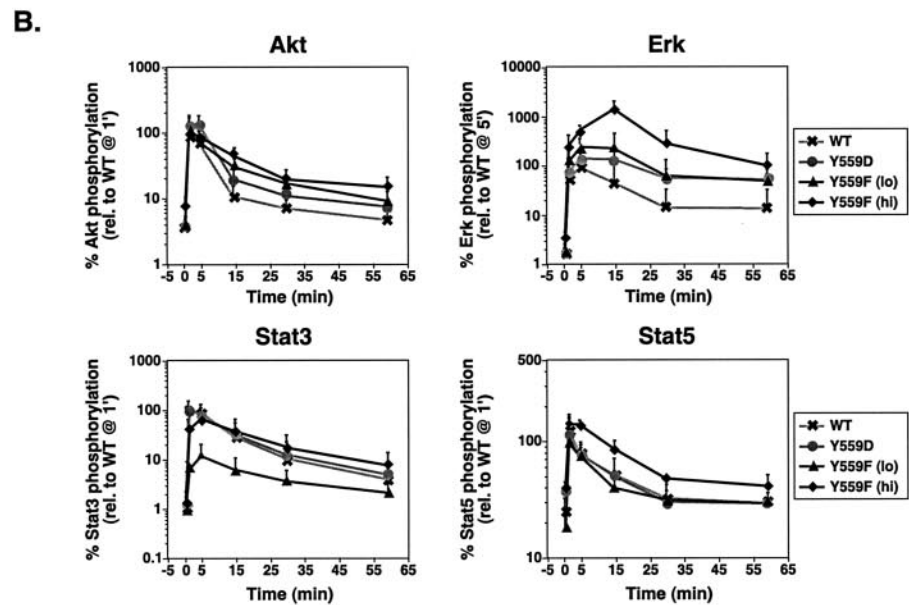


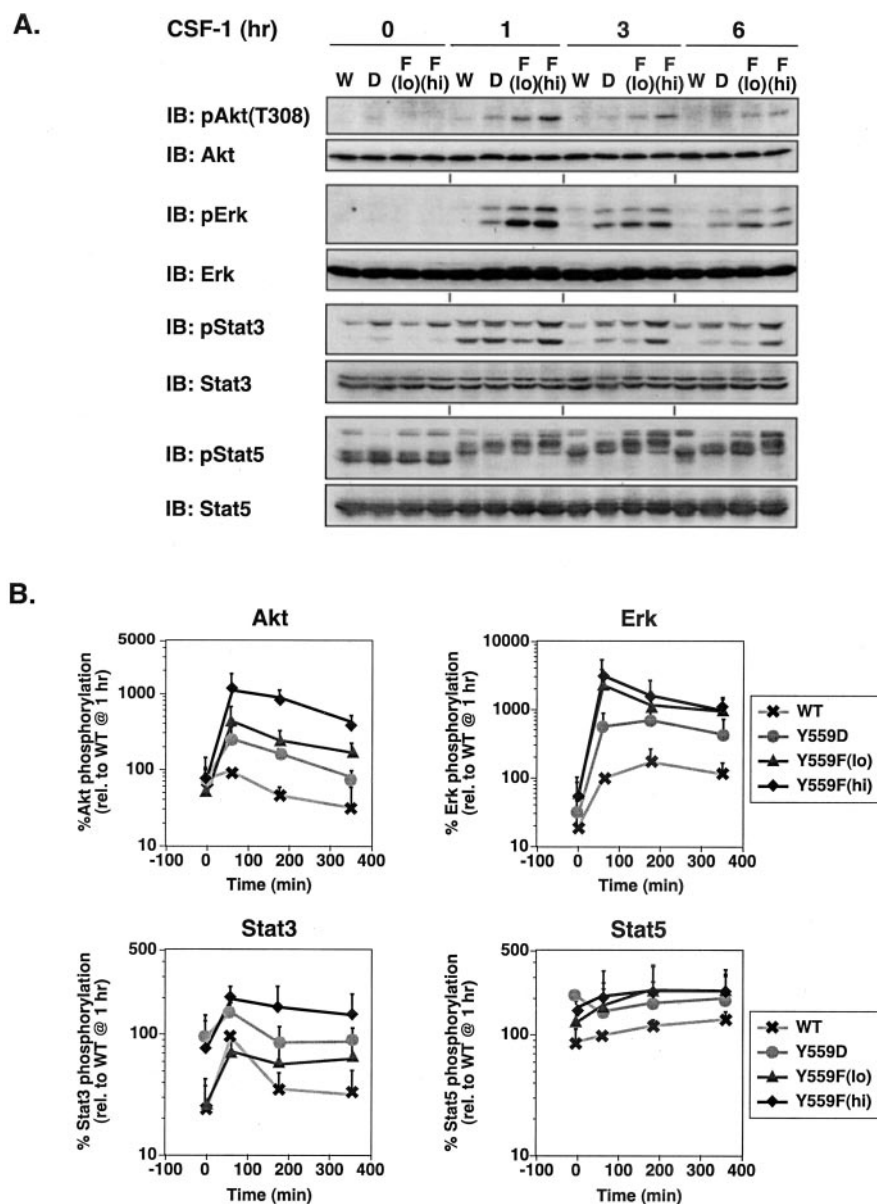
FIG. 4. Positive regulators of cell proliferation and survival downstream of Tyr⁵⁵⁹ mutants. *A*, activation time course for Akt, ERK, and Stat3/5. Cells were stimulated with CSF-1 for the times displayed. TCLs were analyzed by sequential Western blotting with phospho-specific and total protein antibodies as indicated. Shown is a representative of two (Stat5) or three (Akt, ERK, and Stat3) experiments. *B*, quantitation of activation time course. Akt, ERK, Stat3, and Stat5 phosphorylation levels were quantitated and normalized to the corresponding total protein levels. Stat5 quantitation reflects only the band intensity and not the observed mobility shift. The results are displayed as a percent of the maximal WT activation observed for each protein (mean ± S.E.; Akt, ERK, and Stat3, *n* = 3; Stat5, *n* = 2). *C*, increased SHC tyrosine phosphorylation and SHC association with tyrosine-phosphorylated SHIP. Cells were left unstimulated or stimulated with CSF-1 for the indicated times. Lysates were immunoprecipitated with an anti-SHC antibody and analyzed by probing with anti-Tyr(P) antibodies (*top panel*). A parallel blot of TCLs was probed with an anti-SHC antibody as a loading control. Abbreviations in the blots signify: *W*, WT-CSF-1R; *D*, Y559D; *F (lo)*, Y559F (lo); and *F (hi)*, Y559F (hi). *IB*, immunoblot.



a similar time frame (Fig. 4, *A* and *B*). However, we cannot exclude a possible contribution of diminished SHC-associated SHIP tyrosine phosphorylation to the Y559F hyperproliferative phenotype. Collectively, the increased activation of Akt, ERK,

and Stat5 observed in the Y559F mutants despite marked reduction in autophosphorylation, points to a remarkable degree of signal amplification, progressing from the receptor to its downstream effectors.

FIG. 5. Tyr⁵⁵⁹ mutants show persistent activation of downstream pathways. A, extended time course for Akt, ERK, and Stat3/5. The experiment was conducted exactly as described in the legend of Fig. 4, except stimulation was carried out to 6 h. Abbreviations have the same meaning as described in the legend to Fig. 4. B, quantitation of extended time course. Akt, ERK, Stat3, and Stat5 phosphorylation levels were quantitated as described in the legend to Fig. 4. Results are shown as a percent of the WT activation at 1 h (mean \pm S.E., $n = 2$). IB, immunoblot.



Y559 Mutants Show Persistent Activation of Downstream Pathways—While investigating the activation of downstream substrates, we noticed, particularly for the longer time points (15–60 min), a low level of activation that persisted in cells expressing Y559F, compared with cells expressing WT-CSF-1R (Fig. 4, A and B). To further explore this persistent activation, we performed an extended time course experiment. The Y559F mutant, and to a lesser extent the Y559D mutant, showed persistent activation of the Akt, ERK, and Stat5 signaling pathways compared with cells expressing the WT-CSF-1R (Fig. 5, A and B). For Stat3, only the Y559F (hi) clone showed reproducibly increased phosphorylation at the later time points compared with the basal state (Fig. 5, A and B). The low, but persistent activation of downstream pathways may be the cause of the hyperproliferative phenotype observed for the Y559F mutant, and to a lesser extent, the Y559D mutant.

Y559F Exhibits Delayed Receptor Down-regulation—The persistent activation of signaling cascades in cells expressing Y559F could be related to the delay in Y559F receptor degradation that is evident in Fig. 2A. We investigated how the JMD mutations affected receptor internalization and degradation. Cell surface proteins were biotinylated at various times after

CSF-1 stimulation. Total receptor levels were monitored for degradation, whereas biotinylated receptor levels were monitored for internalization. Two controls were performed for the internalization assay to confirm that cells were not lysed during the biotinylation process (data not shown). First, unstimulated cell lysates were biotinylated and the resulting proteins were compared with those from cells lysed after biotinylation. The profiles from these two sets of lysates differed dramatically. Second, we observed no biotinylation of SHP-2, a cytosolic protein, after biotinylation of unbroken cells. CSF-1-stimulated receptor internalization and degradation were reduced in the Y559F mutant (Fig. 6A). Quantitation of receptor degradation showed that even after 90 min, at least 50% of the Y559F receptor remained on the cell surface (Fig. 6B). Y559D exhibited a less pronounced delay in receptor internalization and degradation. Thus, low, but persistent activation of downstream substrates correlates with delayed internalization and degradation of Y559F, whereas the Y559D mutant has a phenotype intermediate between the Y559F and WT receptors.

CSF-1-stimulated CSF-1R Ubiquitination, c-Cbl Phosphorylation, and CSF-1R/c-Cbl Association Are Decreased in Cells Expressing Y559F—c-Cbl, an E3-ubiquitin ligase, is important

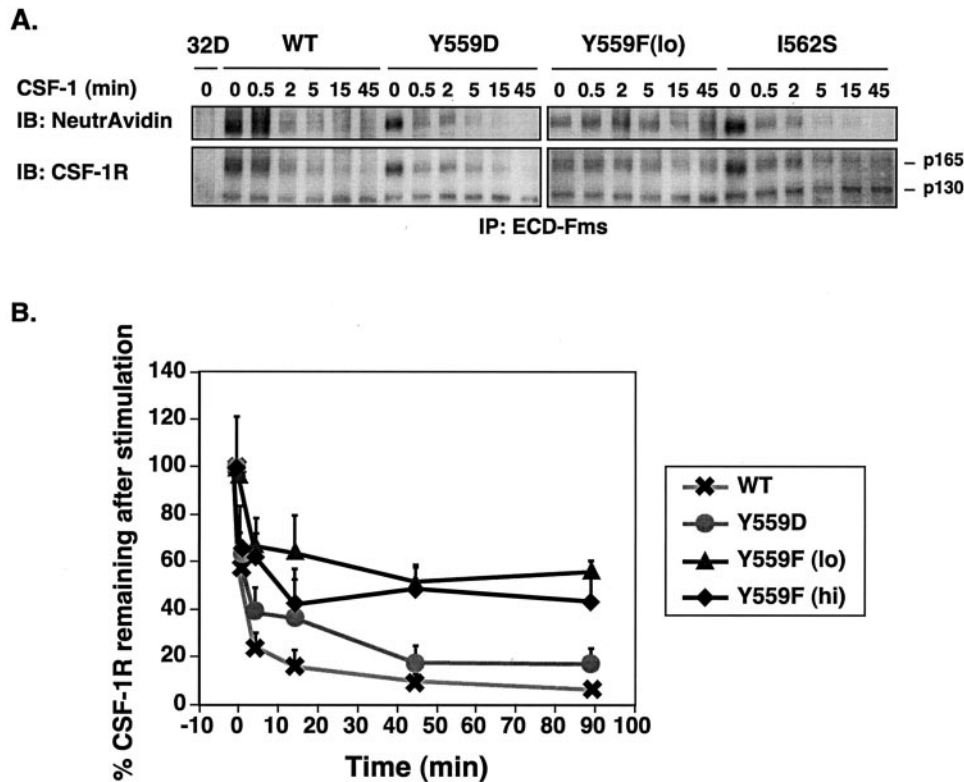


FIG. 6. Y559F exhibits delayed receptor down-regulation. *A*, time course of CSF-1R internalization and degradation. Cells were stimulated with CSF-1 for the indicated times. At each time point, cell surface proteins were labeled with biotin. Lysates were immunoprecipitated with anti-ECD-Fms antibodies and sequentially probed with anti-CSF-1R antibodies and NeutrAvidin-HRP conjugate. Shown is a representative experiment out of three. *B*, quantitation of CSF-1-induced CSF-1R degradation. Results from experiments described in *A* were quantitated. Percent of CSF-1R remaining after stimulation was calculated by dividing the CSF-1R present at each time point by the CSF-1R present in the unstimulated lysate. Shown is the average \pm S.E. ($n = 3$).

for mediating receptor ubiquitination, internalization, and degradation of the CSF-1R (20). c-Cbl is also a substrate for RTKs and tyrosine phosphorylation of c-Cbl may modify its ubiquitin ligase activity (23). Given the critical role of c-Cbl in CSF-1R down-regulation, we next examined the effect of the JMD mutations on indicators of c-Cbl activity. Ubiquitin-specific antibodies were used to probe CSF-1R immunoprecipitates. CSF-1-dependent multiubiquitination was significantly reduced in the Y559F mutant, and less so in Y559D, compared with WT (Fig. 7A). CSF-1-induced c-Cbl tyrosine phosphorylation showed parallel changes for the three receptors (Fig. 7B). One possible reason for the decrease in c-Cbl phosphorylation is a diminished recruitment of c-Cbl to Y559F due to the reduced receptor autophosphorylation. We performed co-immunoprecipitation studies to investigate whether CSF-1-stimulated association of the CSF-1R and c-Cbl was decreased in cells expressing Y559F. Since CSF-1R/c-Cbl co-association is likely to be short-lived because of c-Cbl-induced receptor down-regulation, we conducted preliminary experiments to identify conditions that would stabilize the CSF-1R/c-Cbl association. A proteasome inhibitor (MG-132), lysosome inhibitors (methylamine and chloroquine), and cold temperature (4 °C) were tested. Both cold temperature and chloroquine/MG-132 treatment enhanced WT-CSF-1R and c-Cbl co-association (Fig. 7C). Because cold temperature had the largest effect on preserving CSF-1R/c-Cbl co-association, subsequent experiments were performed at 4 °C. Immunoprecipitates isolated using either anti-c-Cbl (Fig. 7D) or anti-ECD-Fms (Fig. 7E) antibodies showed a clear, CSF-1-dependent association of the CSF-1R and c-Cbl in cells expressing WT-CSF-1R. CSF-1-stimulated co-association was also evident, albeit somewhat reduced, in the Y559D mutant (Fig. 7, *D* and *E*). In contrast, cells expressing Y559F exhibited

little detectable co-association of Y559F and c-Cbl (Fig. 7, *D* and *E*).

Taken together, these findings suggest that the Y559F mutation led to reduced receptor autophosphorylation, presumably including the c-Cbl binding site, and as a consequence, c-Cbl recruitment is diminished. This has the effect of delaying receptor internalization/degradation and prolonging receptor activation signals, leading to hyperproliferation.

DISCUSSION

The goal of this study was to better understand the role played by the JMD in CSF-1R signaling. In particular, we were interested in the function of the SFKs that bind to this domain. Evidence for SFK activation by CSF-1 has previously been established (27). However, the role played by SFKs in CSF-1-mediated signaling remains unclear. Also, recent evidence supports a regulatory role for the JMD in RTK function (40–44). To investigate the significance of SFK recruitment, we established 32Dcl23 clones stably expressing the CSF-1R with point mutations in the SFK binding site. Only mutations at the Tyr⁵⁵⁹ position affected SFK binding upon CSF-1 stimulation. Moreover, cells expressing Y559F, and to a lesser degree Y559D, exhibited markedly reduced CSF-1-stimulated autophosphorylation compared with cells expressing WT-CSF-1R. Remarkably, cells expressing Y559F displayed a hyperproliferative phenotype, most likely due to persistent CSF-1-dependent activation of pro-mitogenic pathways, including Akt, ERK, and Stat5. The prolonged activation of signaling pathways corresponded to a delay in Y559F internalization and degradation. c-Cbl, a ubiquitin ligase, was previously shown to be involved in CSF-1R ubiquitination and down-regulation (20, 65, 66). Several lines of evidence support the conclusion that there is reduced

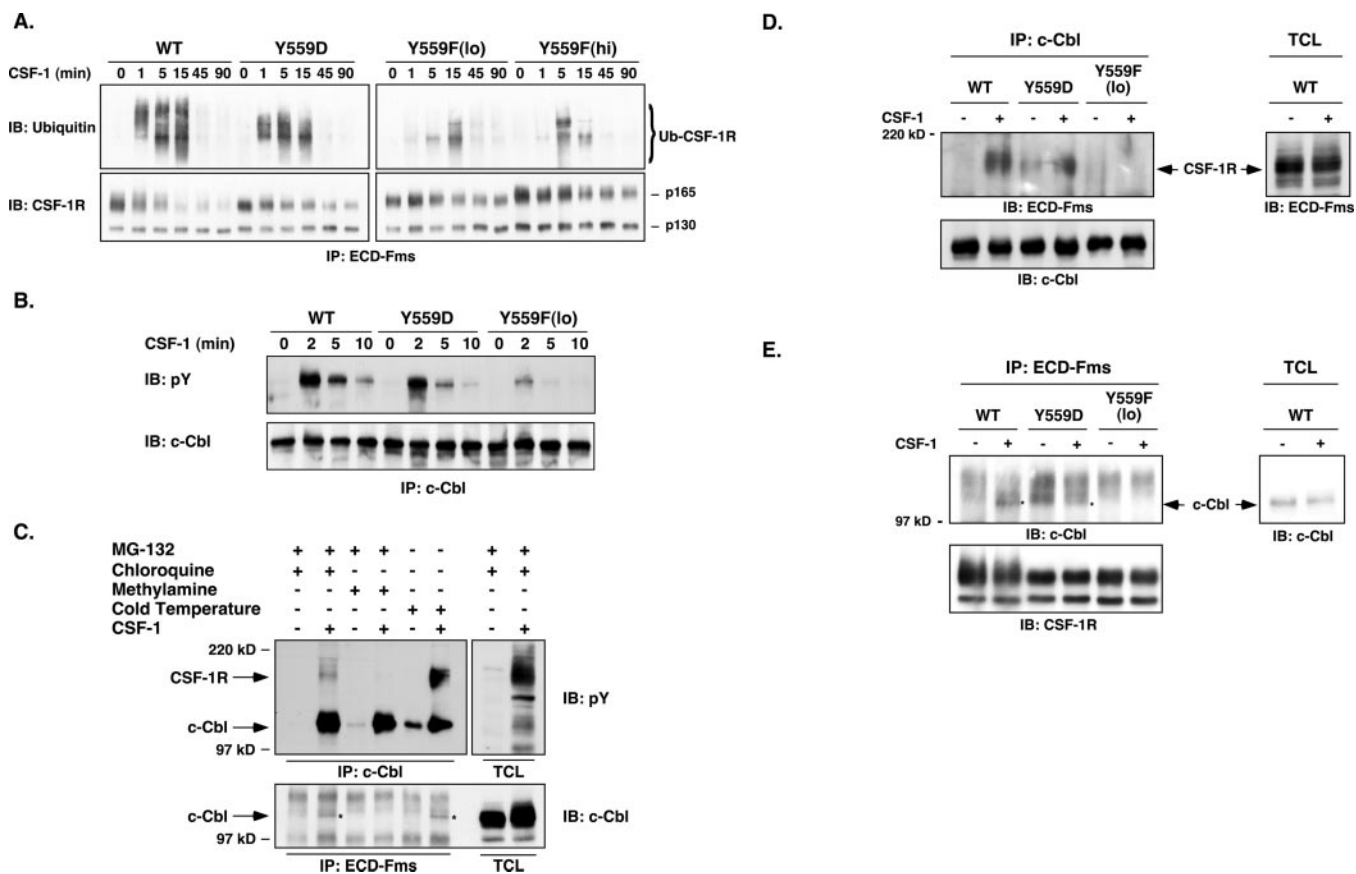


FIG. 7. CSF-1-stimulated receptor ubiquitination, c-Cbl tyrosine phosphorylation, and CSF-1R/c-Cbl co-association are reduced in the Y559F mutant. *A*, CSF-1-induced CSF-1R ubiquitination. Cells were stimulated with CSF-1 for the indicated times. Lysates were immunoprecipitated with anti-ECD-Fms antibodies and sequentially blotted with anti-ubiquitin and anti-CSF-1R antibodies. Results are representative of two experiments. *B*, CSF-1-stimulated c-Cbl tyrosine phosphorylation. Cells were stimulated with CSF-1 for the indicated times. Lysates were immunoprecipitated with anti-c-Cbl antibody and sequentially probed with anti-Tyr(P) and anti-c-Cbl antibodies. Results represent two independent experiments. *C*, CSF-1R/c-Cbl co-association in cells expressing WT-CSF-1R. Cells were treated with the indicated inhibitors 1 h prior to stimulation with CSF-1 at 37 °C, or stimulated with CSF-1 for 20 min at 4 °C. Lysates were immunoprecipitated with anti-c-Cbl or anti-ECD-Fms antibodies. Immunoprecipitates were then probed with anti-Tyr(P) antibodies (anti-c-Cbl immunoprecipitates) or anti-c-Cbl antibodies (anti-ECD-Fms immunoprecipitates). TCLs from unstimulated and stimulated WT clones were loaded onto the same gel and probed for Tyr(P) or c-Cbl to confirm identification. A longer exposure time is shown for the anti-Tyr(P) immunoblot (10 min) relative to TCL blot (2 min). Asterisks indicate the position of the c-Cbl band. *D*, CSF-1R/c-Cbl co-association in c-Cbl immunoprecipitates. Cells were stimulated with CSF-1 at 4 °C for 20 min and lysates were analyzed by anti-c-Cbl immunoprecipitation and anti-ECD-Fms immunoblotting. The blot was stripped and reprobed with anti-c-Cbl antibody. TCL from unstimulated and stimulated WT clones were loaded onto the same gel and probed for CSF-1R. Shown is a representative experiment out of two. The anti-ECD-Fms immunoblot (2.5 min) was exposed for a longer time relative to TCL blot (1 min). *E*, CSF-1R/c-Cbl co-association in CSF-1R immunoprecipitates. Cells were treated as described in *D* and analyzed by anti-ECD-Fms immunoprecipitation and anti-c-Cbl immunoblotting, followed by stripping and reprobing for CSF-1R. TCL from WT clones were loaded onto the same gel and probed for c-Cbl. Results are representative of two experiments. A longer exposure is shown for the TCL blot (3 min) relative to the anti-c-Cbl immunoblot (1 min). Asterisks indicate the position of the c-Cbl band. *IB*, immunoblot.

c-Cbl recruitment to Y559F. CSF-1-induced Y559F multiubiquitination was noticeably diminished. Furthermore, cells expressing Y559F displayed decreased CSF-1-induced tyrosine phosphorylation of c-Cbl and CSF-1R/c-Cbl co-association. We propose a role for reduced c-Cbl binding to Y559F and subsequent delayed down-regulation in mediating the Y559F hyperproliferative phenotype.

Our findings suggest that the JMD in the CSF-1R has multiple functions: in the active state the JMD provides docking sites for signaling molecules such as SFKs and in the inactive state it participates in the regulation of kinase function. Phosphorylation of the SFK binding site in the JMD may serve as a trigger, promoting the transition from an inactive to an active kinase conformation.

The JMD of RTKs was previously thought only to serve as a binding site for interacting proteins (17, 29, 67). Recent literature indicates a more complex role for the JMD. Chan *et al.* (40) showed that the unphosphorylated c-Kit JMD can inhibit its own kinase activity and suppress the transformation of Rat 2 cells expressing an oncogenic c-Kit isoform. Likewise, mutation of the

JMD tyrosines of PDGFR β (54, 67), EphB2 (55), and MuSK (68) decreased receptor autophosphorylation and kinase activity. The significance of the autoinhibitory function of the JMD is also evident from the frequency of c-Kit and Flt3 JMD mutations found in gastrointestinal stromal tumors and acute myeloid leukemias, respectively. Mutations in c-Kit are observed in >90% of gastrointestinal stromal tumors, with 57–71% of these mutations located in the JMD (69), whereas internal tandem duplications in the JMD of Flt3 are found in 15–35% of acute myeloid leukemias and 5–10% of cases of myelodysplasia (70).

The unliganded crystal structures of EphB2 (41) and MuSK (42) as well as Flt3 (43) and c-Kit (44), available recently, provide additional evidence that the JMD maintains the kinase domain in an inactive conformation. The autoinhibited structures of EphB2 and MuSK receptors show the JMD in close proximity to the NH₂-terminal kinase lobe, causing distortion of the α C helix, and in EphB2, the JMD also appears to sterically hinder the activation loop from adopting an active conformation. Compared with EphB2 and MuSK, the JMDs of Flt3 and c-Kit in the inactive structures are even more intimately

associated with the kinase domain, as portions of the JMD are buried in the interface between the NH₂- and COOH-terminal kinase lobes. The regulatory tyrosines of c-Kit and Flt3 in their unphosphorylated state seem to stabilize the JMD and kinase domain interactions. In support of this, the JMD in the active c-Kit structure adopts a very different conformation, with the phosphorylated tyrosines interacting in *trans* with the kinase active center (45). Interestingly, mass spectrometry analysis of c-Kit autophosphorylation indicates that Tyr⁵⁶⁸/Tyr⁵⁷⁰ of the JMD are the first tyrosines to be phosphorylated (45), reflecting their importance in regulating the autoinhibited state. On the other hand, our data demonstrating that Y559F can be phosphorylated *in vitro* suggest that the JMD tyrosines are not absolutely required for kinase activity.

We have modeled the mouse CSF-1R juxtamembrane and kinase domains (minus the KI) using the autoinhibited human Flt3 structure as a template (Fig. 8), as the coordinates of the c-Kit structure had not been released at the time of manuscript preparation. Because of the more limited sequence homology in the NH₂-terminal portion of the JMD between Flt3 and the CSF-1R, the first 8 amino acids (Tyr⁵⁴⁴–Ile⁵⁵¹) in the CSF-1R are not present. Otherwise, the Flt3 (Fig. 8A) and CSF-1R (Fig. 8B) structures are almost completely superimposable and the close proximity of the YTFI motif to the kinase lobe is clearly evident. It is likely that the CSF-1R JMD functions in a manner similar to that proposed for c-Kit and Flt3. By preventing Tyr⁵⁵⁹ phosphorylation, the Y559F mutant will be locked into a relatively autoinhibited conformation. This results in reduced, but not absent, kinase activity and autophosphorylation. Thus, Tyr⁵⁵⁹ serves as a phosphorylation switch in the regulation of kinase activity. In light of this finding, conclusions about SFK function in CSF-1R signaling that used Tyr to Phe substitutions in the SFK binding site may need to be re-examined.

RTK activation signals both positive and negative effectors and it is the balance between these signals that determines the response to ligand stimulation (71). Our results confirm the importance of this balance, as despite reduced receptor autophosphorylation, the Y559F mutant exhibited a hyperproliferative phenotype, suggesting a disruption of negative regulation. Deregulation of signaling from negative effectors is an important mechanism for cellular transformation (8). For example, a Tyr to Phe substitution at Tyr⁵⁶⁹ in the c-Kit JMD, which disrupts binding of SHP-1, a protein-tyrosine phosphatase involved in RTK negative regulation, induces a ligand-dependent hyperproliferative response (72). Another example of RTK negative regulation is receptor down-regulation (73). An internalization-defective EGFR induced a transformed phenotype and anchorage-independent growth of NR6 cells in response to low ligand concentrations compared with cells expressing WT-EGFR (74). Unregulated receptor function is also found in the viral form of the CSF-1R, *v-fms*. One alteration of *v-fms* is replacement of the CSF-1R carboxyl terminus (50 amino acids), including the c-Cbl binding site, with 14 unrelated amino acids (16). This prohibits regulation of *v-fms* endocytosis by c-Cbl-dependent ubiquitination. However, when the c-Cbl binding site is fused to *v-fms*, its transforming ability is decreased (15).

Our results also highlight a critical role for defective receptor down-regulation in mediating the Y559F hyperproliferative phenotype (Fig. 6). As Lee *et al.* (20) have shown that c-Cbl is important for mediating CSF-1R ubiquitination and degradation, we investigated a connection between delayed Y559F down-regulation and c-Cbl. Supporting such a connection, delayed Y559F down-regulation correlated with reduced Y559F multi-ubiquitination. Furthermore, decreased c-Cbl phosphorylation mediated by the Y559F mutant as well as reduced CSF-1R/c-Cbl co-association demonstrate that c-Cbl was not recruited to Y559F

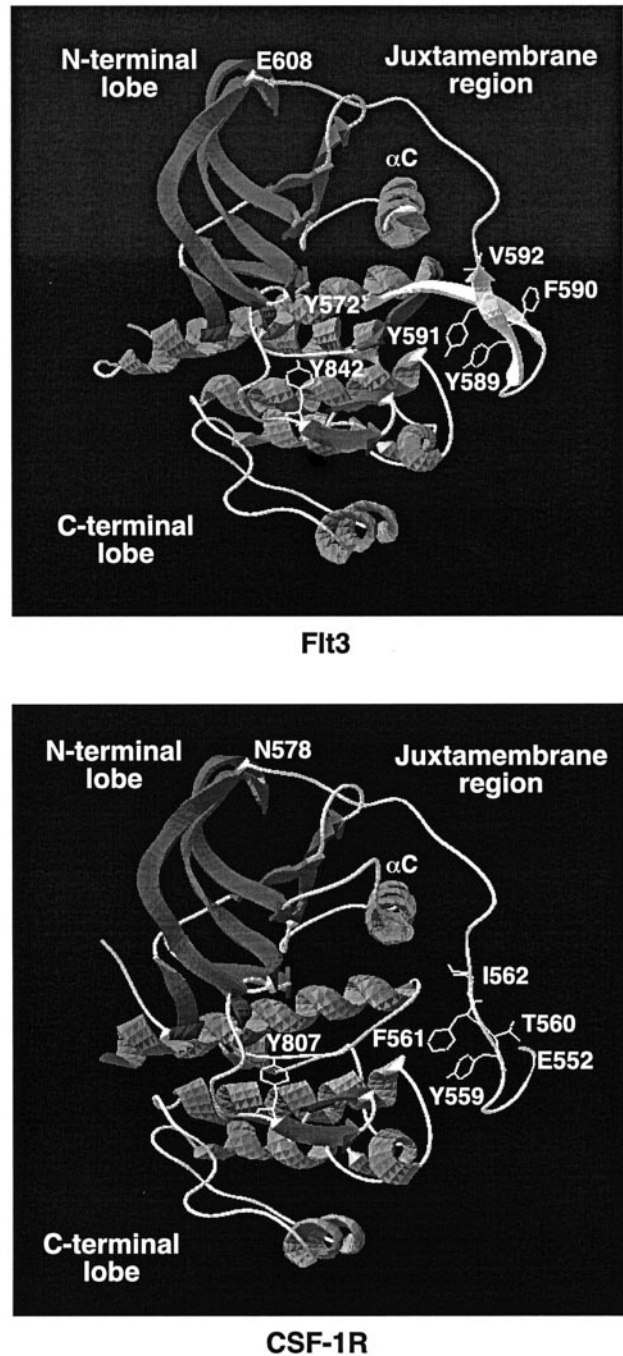


FIG. 8. Model of the autoinhibited CSF-1R structure. A, Flt3 structure. Structure of the autoinhibited human Flt3 receptor (Protein Data Bank code 1RJB) lacking the KI. The JMD is located between Tyr⁵⁷² and Glu⁶⁰⁸. The SFK binding site and activation loop tyrosine amino acids are marked. B, CSF-1R model. Structure of the autoinhibited mouse CSF-1R without the KI, modeled on the autoinhibited Flt3 structure (see "Materials and Methods"). The JMD is situated between Glu⁵⁵² and Asn⁵⁷⁸. The SFK binding motif and activation loop tyrosine are indicated.

as efficiently as to WT-CSF-1R. This is most likely due to the reduced autophosphorylation exhibited by cells expressing Y559F. Tyr⁹⁷⁴ phosphorylation has been shown to be necessary for c-Cbl binding, but there is no data indicating that it is sufficient (15, 16). Although we did not specifically examine phosphorylation of Tyr⁹⁷⁴, it is likely that phosphorylation of this residue is also reduced, as CSF-1R immunoprecipitates probed by two (Tyr)P-specific antibodies (4G10 and PY99) and phospho-Tyr⁸⁰⁷ CSF-1R antibody showed diminished receptor phosphorylation

(Fig. 2). However, our results cannot rule out a more direct role for the JMD in c-Cbl recruitment.

The decrease in receptor down-regulation provides an explanation for the Y559F hyperproliferative phenotype. Namely, reduced c-Cbl recruitment and activation results in decreased Y559F multiubiquitination and a delay in receptor down-regulation. The ensuing low, but persistent pro-mitogenic signals were sufficient to support enhanced cell growth. However, we cannot exclude the involvement of a second unidentified regulator. This regulator could be an activator of proliferation, which is recruited by the Y559F mutant, or it could be a negative regulator, whose recruitment to the CSF-1R is diminished in the Y559F mutant. Although we have not directly shown a connection between c-Cbl and hyperproliferation, there is evidence for this hypothesis in the literature. First, bone marrow macrophages lacking c-Cbl display a significant increase in cell proliferation compared with wild-type macrophages (20). Second, exogenous expression of c-Met with a mutated c-Cbl binding site causes an increase in fibroblast transformation (75). Third, overexpression of c-Cbl in cells exogenously expressing the PDGFR α results in decreased ligand-induced cell proliferation (37). Together, our results support the idea that disruption of c-Cbl down-regulation of RTKs is important for oncogenic transformation (76).

Signaling responses initiated by activated RTKs located on endosomes has been proposed to sustain, activate, or amplify the receptor response (77). Evidence for this largely comes from EGFR studies. For example, certain signaling molecules such as SHC were complexed to the EGFR in endosomes (78). In addition, using a specific EGFR inhibitor and the receptor recycling inhibitor monensin, Wang *et al.* (79) demonstrated that endosomal EGFR activation initiated activation of Ras, ERK, and Akt and suppressed serum withdrawal-stimulated apoptosis. However, our results indicate that CSF-1R internalization and degradation are closely coupled and it is unlikely that enhanced endosomal signaling is responsible for the Y559F hyperproliferative phenotype.

In conclusion, we have demonstrated a complex role for the JMD in CSF-1R signaling involving regulation of SFK binding, kinase domain function, and indirectly, receptor down-regulation. These findings may have implications for other RTKs and in particular may provide insight into gain-of-function mutations of c-Kit and Flt3 found in various tumors.

Acknowledgments—We acknowledge Mike Hayes for technical assistance in establishing the 32D stable cell lines and obtaining the growth data shown in Fig. 3, A–C. We thank David States and members of the Lee lab for helpful discussions and suggestions. In addition, we appreciate the generosity of Marilyn D. Resh and Arthur Nienhuis for reagents and the Genetics Institute for the human rCSF-1.

REFERENCES

- Stanley, E. R., Berg, K. L., Einstein, D. B., Lee, P. S., Pixley, F. J., Wang, Y., and Yeung, Y. G. (1997) *Mol. Reprod. Dev.* **46**, 4–10
- Hamilton, J. A. (1997) *J. Leukocyte Biol.* **62**, 145–155
- Rohrschneider, L. R., Bourette, R. P., Lioubin, M. N., Algate, P. A., Myles, G. M., and Carlberg, K. (1997) *Mol. Reprod. Dev.* **46**, 96–103
- Felix, R., Cecchini, M. G., and Fleisch, H. (1990) *Endocrinology* **127**, 2592–2594
- Wiktor-Jedrzejczak, W., Bartocci, A., Ferrante, A. W. Jr., Ahmed-Ansari, A., Sell, K. W., Pollard, J. W., and Stanley, E. R. (1990) *Proc. Natl. Acad. Sci. U. S. A.* **87**, 4828–4832
- Yoshida, H., Hayashi, S., Kunisada, T., Ogawa, M., Nishikawa, S., Okamura, H., Sudo, T., and Shultz, L. D. (1990) *Nature* **345**, 442–444
- Dai, X. M., Ryan, G. R., Hapel, A. J., Dominguez, M. G., Russell, R. G., Kapp, S., Sylvestre, V., and Stanley, E. R. (2002) *Blood* **99**, 111–120
- Blume-Jensen, P., and Hunter, T. (2001) *Nature* **411**, 355–365
- Bourette, R. P., and Rohrschneider, L. R. (2000) *Growth Factors* **17**, 155–166
- Davis, J. N., Rock, C. O., Cheng, M., Watson, J. B., Ashmun, R. A., Kirk, H., Kay, R. J., and Roussel, M. F. (1997) *Mol. Cell. Biol.* **17**, 7398–7406
- van der Geer, P., and Hunter, T. (1993) *EMBO J.* **12**, 5161–5172
- Bourette, R. P., Arnaud, S., Myles, G. M., Blanchet, J. P., Rohrschneider, L. R., and Mouchiroud, G. (1998) *EMBO J.* **17**, 7273–7281
- Reedijk, M., Liu, X., van der Geer, P., Letwin, K., Waterfield, M. D., Hunter, T., and Pawson, T. (1992) *EMBO J.* **11**, 1365–1372
- Novak, U., Nice, E., Hamilton, J. A., and Paradiso, L. (1996) *Oncogene* **13**, 2607–2613
- Mancini, A., Koch, A., Wilms, R., and Tamura, T. (2002) *J. Biol. Chem.* **277**, 14635–14640
- Wilhelmsen, K., Burkhalter, S., and van der Geer, P. (2002) *Oncogene* **21**, 1079–1089
- Alonso, G., Koegl, M., Mazurenko, N., and Courtneidge, S. A. (1995) *J. Biol. Chem.* **270**, 9840–9848
- Mancini, A., Nienthal, R., Joos, H., Koch, A., Trouliaris, S., Niemann, H., and Tamura, T. (1997) *Oncogene* **15**, 1565–1572
- Joos, H., Trouliaris, S., Helftenbein, G., Niemann, H., and Tamura, T. (1996) *J. Biol. Chem.* **271**, 24476–24481
- Lee, P. S., Wang, Y., Dominguez, M. G., Yeung, Y. G., Murphy, M. A., Bowtell, D. D., and Stanley, E. R. (1999) *EMBO J.* **18**, 3616–3628
- Joazeiro, C. A., Wing, S. S., Huang, H., Levenson, J. D., Hunter, T., and Liu, Y. C. (1999) *Science* **286**, 309–312
- Ceresa, B. P., and Schmid, S. L. (2000) *Curr. Opin. Cell Biol.* **12**, 204–210
- Levkowitz, G., Waterman, H., Ettenberg, S. A., Katz, M., Tsygankov, A. Y., Alroy, I., Lavi, S., Iwai, K., Reiss, Y., Ciechanover, A., Lipkowitz, S., and Yarden, Y. (1999) *Mol. Cell* **4**, 1029–1040
- Soubeyran, P., Kowanetz, K., Szymkiewicz, I., Langdon, W. Y., and Dikic, I. (2002) *Nature* **416**, 183–187
- Petrelli, A., Gilestro, G. F., Lanzardo, S., Comoglio, P. M., Migone, N., and Giordano, S. (2002) *Nature* **416**, 187–190
- Lee, A. W., and States, D. J. (2000) *Mol. Cell. Biol.* **20**, 6779–6798
- Courtneidge, S. A., Dhand, R., Pilat, D., Twamley, G. M., Waterfield, M. D., and Roussel, M. F. (1993) *EMBO J.* **12**, 943–950
- Kypta, R. M., Goldberg, Y., Ulug, E. T., and Courtneidge, S. A. (1990) *Cell* **62**, 481–492
- Linnekin, D., DeBerry, C. S., and Mou, S. (1997) *J. Biol. Chem.* **272**, 27450–27455
- Osherov, N., and Levitzki, A. (1994) *Eur. J. Biochem.* **225**, 1047–1053
- Bondzi, C., Litz, J., Dent, P., and Krystal, G. W. (2000) *Cell Growth Differ.* **11**, 305–314
- Marks, D. C., Csar, X. F., Wilson, N. J., Novak, U., Ward, A. C., Kanagasundaram, V., Hoffmann, B. W., and Hamilton, J. A. (1999) *Mol. Cell. Biol. Res. Commun.* **1**, 144–152
- Wang, Y. Z., Wharton, W., Garcia, R., Kraker, A., Jove, R., and Pledger, W. J. (2000) *Oncogene* **19**, 2075–2085
- Courtneidge, S. A. (2002) *Biochem. Soc. Trans.* **30**, 11–17
- DeMali, K. A., Godwin, S. L., Soltoff, S. P., and Kazlauskas, A. (1999) *Exp. Cell Res.* **253**, 271–279
- Baran, C. P., Tridandapani, S., Helgason, C. D., Humphries, R. K., Krystal, G., and Marsh, C. B. (2003) *J. Biol. Chem.* **278**, 38628–38636
- Rosenkrantz, S., Ikuno, Y., Leong, F. L., Klinghoffer, R. A., Miyake, S., Band, H., and Kazlauskas, A. (2000) *J. Biol. Chem.* **275**, 9620–9627
- Myles, G. M., Brandt, C. S., Carlberg, K., and Rohrschneider, L. R. (1994) *Mol. Cell. Biol.* **14**, 4843–4854
- Scheijen, B., and Griffin, J. D. (2002) *Oncogene* **21**, 3314–3333
- Chan, P. M., Ilangumaran, S., La Rose, J., Chakrabarty, A., and Rottapel, R. (2003) *Mol. Cell. Biol.* **23**, 3067–3078
- Wybenga-Groot, L. E., Baskin, B., Ong, S. H., Tong, J., Pawson, T., and Sicheri, F. (2001) *Cell* **106**, 745–757
- Till, J. H., Becerra, M., Watty, A., Lu, Y., Ma, Y., Neubert, T. A., Burden, S. J., and Hubbard, S. R. (2002) *Structure (Lond.)* **10**, 1187–1196
- Griffith, J., Black, J., Faerman, C., Swenson, L., Wynn, M., Lu, F., Lippe, J., and Saxena, K. (2004) *Mol. Cell* **13**, 169–178
- Mol, C. D., Dougan, D. R., Schneider, T. R., Skene, R. J., Kraus, M. L., Scheibe, D. N., Snell, G. P., Zou, H., Sang, B., and Wilson, K. P. (2004) *J. Biol. Chem.* **279**, 31655–31663
- Mol, C. D., Lim, K. B., Sridhar, V., Zou, H., Chien, E. Y. T., Sang, B., Nowakowski, J., Kassel, D. B., Cronin, C. N., and McRee, D. E. (2003) *J. Biol. Chem.* **278**, 31461–31464
- Lee, A. W. (1999) *Blood* **93**, 537–553
- Lee, A. W., and Nienhuis, A. W. (1992) *J. Biol. Chem.* **267**, 16472–16483
- Ota, J., Sato, K., Kimura, F., Wakimoto, N., Nakamura, Y., Nagata, N., Suzu, S., Yamada, M., Shimamura, S., and Motoyoshi, K. (2000) *FEBS Lett.* **466**, 96–100
- Peitsch, M. C. (1995) *Bio/Technology* **13**, 658–660
- Guex, N., and Peitsch, M. C. (1997) *Electrophoresis* **18**, 2714–2723
- Schuede, T., Kopp, J., Guex, N., and Peitsch, M. C. (2003) *Nucleic Acids Res.* **31**, 3381–3385
- Irusta, P. M., and DiMaio, D. (1998) *EMBO J.* **17**, 6912–6923
- Irusta, P. M., Luo, Y., Bakht, O., Lai, C. C., Smith, S. O., and DiMaio, D. (2002) *J. Biol. Chem.* **277**, 38627–38634
- Baxter, R. M., Secrist, J. P., Vaillancourt, R. R., and Kazlauskas, A. (1998) *J. Biol. Chem.* **273**, 17050–17055
- Binns, K. L., Taylor, P. P., Sicheri, F., Pawson, T., and Holland, S. J. (2000) *Mol. Cell. Biol.* **20**, 4791–4805
- Waksman, G., Shoelson, S. E., Pant, N., Cowburn, D., and Kuriyan, J. (1993) *Cell* **72**, 779–790
- Songyang, Z., Shoelson, S. E., Chaudhuri, M., Gish, G., Pawson, T., Haser, W. G., King, F., Roberts, T., Ratnofsky, S., Lechleider, R. J., Neel, B., Birge, R., Fajardo, J., Chou, M., Hanafusa, H., Shaffhausen, B., and Cantley, L. C. (1993) *Cell* **72**, 767–778
- Hubbard, S. R., Mohammadi, M., and Schlessinger, J. (1998) *J. Biol. Chem.* **273**, 11987–11990
- Blake, R. A., Broome, M. A., Liu, X., Wu, J., Gishizky, M., Sun, L., and Courtneidge, S. A. (2000) *Mol. Cell. Biol.* **20**, 9018–9027
- Rane, S. G., and Reddy, E. P. (2002) *Oncogene* **21**, 3334–3358
- Decker, T., and Kovarik, P. (2000) *Oncogene* **19**, 2628–2637
- Schreiner, S. J., Schiavone, A. P., and Smithgall, T. E. (2002) *J. Biol. Chem.* **277**, 45680–45687
- Gotoh, N., Tojo, A., Muroya, K., Hashimoto, Y., Hattori, S., Nakamura, S.,

- Takenawa, T., Yazaki, Y., and Shibuya, M. (1994) *Proc. Natl. Acad. Sci. U. S. A.* **91**, 167–171
64. Lioubin, M. N., Algate, P. A., Tsai, S., Carlberg, K., Aebersold, A., and Rohrschneider, L. R. (1996) *Genes Dev.* **10**, 1084–1095
65. Wang, Y., Yeung, Y. G., Langdon, W. Y., and Stanley, E. R. (1996) *J. Biol. Chem.* **271**, 17–20
66. Wang, Y., Yeung, Y. G., and Stanley, E. R. (1999) *J. Cell. Biochem.* **72**, 119–134
67. Mori, S., Ronnstrand, L., Yokote, K., Engstrom, A., Courtneidge, S. A., Claesson-Welsh, L., and Heldin, C. H. (1993) *EMBO J.* **12**, 2257–2264
68. Herbst, R., and Burden, S. J. (2000) *EMBO J.* **19**, 67–77
69. Duffaud, F., and Blay, J. Y. (2003) *Oncology* **65**, 187–197
70. Stirewalt, D. L., and Radich, J. P. (2003) *Nat. Rev. Cancer* **3**, 650–665
71. Dikic, I., and Giordano, S. (2003) *Curr. Opin. Cell Biol.* **15**, 128–135
72. Kozlowski, M., Larose, L., Lee, F., Le, D. M., Rottapel, R., and Siminovitch, K. A. (1998) *Mol. Cell. Biol.* **18**, 2089–2099
73. Sorkin, A., and Von Zastrow, M. (2002) *Nat. Rev. Mol. Cell. Biol.* **3**, 600–614
74. Wells, A., Welsh, J. B., Lazar, C. S., Wiley, H. S., Gill, G. N., and Rosenfeld, M. G. (1990) *Science* **247**, 962–964
75. Peschard, P., Fournier, T. M., Lamorte, L., Naujokas, M. A., Band, H., Langdon, W. Y., and Park, M. (2001) *Mol. Cell* **8**, 995–1004
76. Peschard, P., and Park, M. (2003) *Cancer Cell* **3**, 519–523
77. Wiley, H. S., and Burke, P. M. (2001) *Traffic* **2**, 12–18
78. Burke, P., Schooler, K., and Wiley, H. S. (2001) *Mol. Biol. Cell* **12**, 1897–1910
79. Wang, Y., Pennock, S., Chen, X., and Wang, Z. (2002) *Mol. Cell. Biol.* **22**, 7279–7290